Crystal Structure of a TOG Domain: Conserved Features of XMAP215/Dis1-Family TOG Domains and Implications for Tubulin Binding

Jawdat Al-Bassam,[1] Nicholas A. Larsen,[1] Anthony A. Hyman,[3] and Stephen C. Harrison[1,2,*]
[1] Jack and Eileen Connors Laboratory of Structural Biology
[2] Howard Hughes Medical Institute
Harvard Medical School, Boston, MA 02115, USA
[3] Max Planck Institute of Molecular Cell Biology and Genetics, 01307 Dresden, Germany
*Correspondence: harrison@crystal.harvard.edu
DOI 10.1016/j.str.2007.01.012

SUMMARY

Members of the XMAP215/Dis1 family of microtubule-associated proteins (MAPs) are essential for microtubule growth. MAPs in this family contain several 250 residue repeats, called TOG domains, which are thought to bind tubulin dimers and promote microtubule polymerization. We have determined the crystal structure of a single TOG domain from the *Caenorhabditis elegans* homolog, Zyg9, to 1.9 Å resolution, and from it we describe a structural blueprint for TOG domains. These domains are flat, paddle-like structures, composed of six HEAT-repeat elements stacked side by side. The two wide faces of the paddle contain the HEAT-repeat helices, and the two narrow faces, the intra- and inter-HEAT repeat turns. Solvent-exposed residues in the intrarepeat turns are conserved, both within a particular protein and across the XMAP215/Dis1 family. Mutation of some of these residues in the TOG1 domain from the budding yeast homolog, Stu2p, shows that this face indeed participates in the tubulin contact.
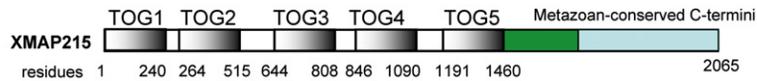
INTRODUCTION

Microtubules are dynamic cytoskeletal structures that undergo alternate phases of growth and shrinkage. During growth, tubulin αβ-heterodimers associate onto microtubule ends; individual microtubules then switch stochastically to dissociation and shrinkage. The transitions between phases are known as "catastrophe" (growth to shrinkage) and "rescue" (shrinkage to growth), respectively. This dynamic instability is essential for the rapid reorganization of the microtubule cytoskeleton during mitosis (reviewed in Desai and Mitchison, 1997).

The XMAP215/Dis1 group of proteins is the only microtubule-associated protein (MAP) family with representative orthologs in fungi, plants, and animals. All its members
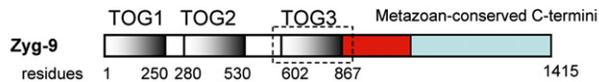
are essential for correct microtubule dynamics during cell division (Ohkura et al., 2001; Kinoshita et al., 2002). Conservation of primary structure among the XMAP215/Dis1 family members is restricted to their N-terminal regions, which contain two to five so-called "TOG domains," named after their initial identification in the human ortholog, ch-TOG (Charrasse et al., 1998). There are three design plans for XMAP215/Dis1 proteins based on the number of TOG domains they contain (Figure 1): (1) higher eukaryotic homologs, such as *Xenopus laevis* XMAP215, *Arabidopsis thaliana* MOR1, and human ch-TOG contain five TOG domains—the proteins are likely to be monomeric (Figure 1A; Kinoshita et al., 2005); (2) *Caenorhabditis elegans* Zyg9 (and other nematode orthologs) contain three TOG domains (Figure 1B); (3) lower eukaryotic homologs, such as *Saccharomyces cerevisiae* Stu2p and *Schizosaccharomyces pombe* Dis1p or Alp14p, contain two TOG domains near their N termini and form homodimers through coiled-coil segments near their C termini (Figure 1C; Al-Bassam et. al., 2006). The domains fall into classes based on their position in each XMAP215/Dis1 sequence. TOG domains of any one class are more similar to each other than to members of other classes (Gard et al., 2004). Their structures are predicted to contain HEAT repeats (Huntingtin, Elongation factor-3, A subunit of PR65, Tor-kinase repeats), α-helical zig-zags that stack to form elongated, sometimes spirally curved domains (reviewed in Ohkura et al., 2001).

Individual XMAP215/Dis1 family proteins exhibit a puzzling diversity of functional properties. Most family members have microtubule-stabilizing activity (reviewed in Ohkura et al., 2001; Severin et al., 2001; Gergely et al., 2003; Cassimeris and Morabito, 2004; Holmfeldt et al., 2004; Tournebize et al., 2000; Garcia et al., 2001; Nakaseko et al., 2001; Gräf et al., 2003; Whittington et al., 2001). They increase microtubule plus-end growth rates, suggesting that they facilitate plus-end addition of αβ-tubulin heterodimers (Gard and Kirschner, 1987; Vasquez et al., 1994). XMAP215/Dis1 proteins can also have destabilizing activity in some experimental contexts. Examples of the latter are Stu2p (Kosco et al., 2001; van Breugel et al., 2003; Usui et al., 2003), ch-TOG (Holmfeldt et al.,

A Higher Eukaryotes

B Nematode

C Yeast

Figure 1. Domain Organization of XMAP215/Dis1 Proteins

(A) XMAP215 represents the higher eukaryotic orthologs, with five TOG domains. A variable region (green) connects TOG5 to a conserved, C-terminal region of unknown structure (light blue).

(B) Zyg9 represents the nematode ortholog of XMAP215, with three TOG domains. A variable region (red) connects TOG3 to the conserved C-terminal region (light blue).

(C) Stu2p represents homologs found in both budding and fission yeast. It contains TOG1 and TOG2, followed by a basic linker and a coil-coil for homodimerization.

2004), and XMAP215 (Shirasu-Hiza et al., 2003). Msps, another family member, acts as an antipause factor (Brittle and Ohkura, 2005).

One possible explanation for these differences comes from the finding that Stu2p fragments, containing either just the first or both of its TOG domains, bind unpolymerized αβ-tubulin heterodimers (Al-Bassam et al., 2006). Homodimeric Stu2p captures free tubulin very tightly; in the process, it undergoes a conformational change from an "open" structure, with flexibly linked TOG domains, to a "closed" structure, with the two sets of TOG domains encircling a single tubulin heterodimer (Al-Bassam et al., 2006). Higher eukaryotic XMAP215/Dis1 proteins also bind free tubulin (T. Notzel, A.A.H., and J.A.-B., unpublished data). Thus, capture of tubulin heterodimers is a general property of TOG-domain proteins. Consistent with this mechanism are recent in vitro, high-resolution tracking experiments, which show that microtubule growth in the presence of XMAP215 is saltatory (Kerssemakers et al., 2006). The high affinity of TOG domains for tubulin could lead to either removal or addition of tubulin subunits at microtubule ends, depending on free tubulin concentration and on many other variable intracellular or experimental factors. We have not yet been able to test this notion directly, because the structural basis of the interaction is unknown.

We have determined a crystal structure of the third TOG domain from *C. elegans* Zyg-9 at 1.9 Å resolution. The Zyg9-TOG3 structure shows that a TOG-domain core has six conserved HEAT repeats. The domain has a flat, paddle-like shape; the two wide faces are lined by the "A" and "B" helices of the HEAT repeats, respectively, and the two narrow faces by the intra- and inter-HEAT repeat turns. Sequence alignment of TOG domains shows conservation in two types of residues: hydrophobic residues that determine inter-HEAT repeat stacking, and solvent exposed residues in the turns between A and B helices of HEAT repeats 1–5. The side chains in these intrarepeat turns form a 39 Å long, continuous patch on a single, narrow face of the TOG-domain structure. Mutation of conserved residues in these turns reduces the affinity of Stu2-TOG1 for tubulin dimer in solution, showing that they indeed are part of a recognition surface for unpolymerized tubulin.

RESULTS AND DISCUSSION

Structure of Zyg9 TOG3

Zyg9 TOG3 has seven HEAT repeats (Figure 1). Each repeat is an α-helical zig-zag, and the individual helices, designated A and B, are 15–20 residues in length. The core of the structure contains repeats HR1-HR6 (Figure 2, blue helices), aligned roughly parallel to each other. The N-terminal repeat (HR0; Figure 2, red helices) packs alongside HR1 and HR2. It thus lies outside the principal stack. Unlike Zyg9 TOG3, most HEAT-repeat-containing structures have marked curvature (Cingolani et al., 1999). HR1 to HR3 and HR4 to HR5 indeed pack with a modest, right-hand twist, as seen in other HEAT-repeat proteins, but a left-hand packing between HR3 and HR4 restores parallelism and produces a flat, paddle-like domain. The two wide faces of the paddle are formed by the A and B helices; the two narrow faces, by the intrarepeat and interrepeat turns (T1-2 to T4-5). HR6 packs onto HR5 with a 45° right-hand twist, thus placing its intra-HEAT repeat turn on the wide face of the paddle. The N and C termini extend from opposite ends of the paddle-like structure.

### Conserved Features of TOG Domains

In Figure 3 is an alignment of TOG-domain sequences from *X. laevis* XMAP215 (five TOG domains), *C. elegans* Zyg9 (three TOG domains), and budding yeast Stu2p (two TOG domains). Alignments with a larger group of TOG-domain sequences lead to the same conclusions we draw from this set. We grouped residues into three categories, depending on their degree of conservation: highly conserved, if a residue is invariant or if it retains its size and charge in 100% of the sequences (Figure 3, purple); moderately conserved, if a residue retains its size and charge in more than 70% of the sequences (Figure 3, blue); and weakly conserved, if a residue retains its size and charge in 30% of sequences (Figure 3, cyan). The HR0 sequence (Figures 2 and 3, red helices) is present only in XMAP215 TOG5 and Zyg9 TOG3 (as well as the fifth TOG domains of MOR1, Msps, and other orthologs from higher eukaryotes). In the other TOG domain sequences, HR0 is replaced by proline- and glycine-rich segments, which are not conserved, and which are likely to adopt nonhelical conformations. There is clear evidence of conservation
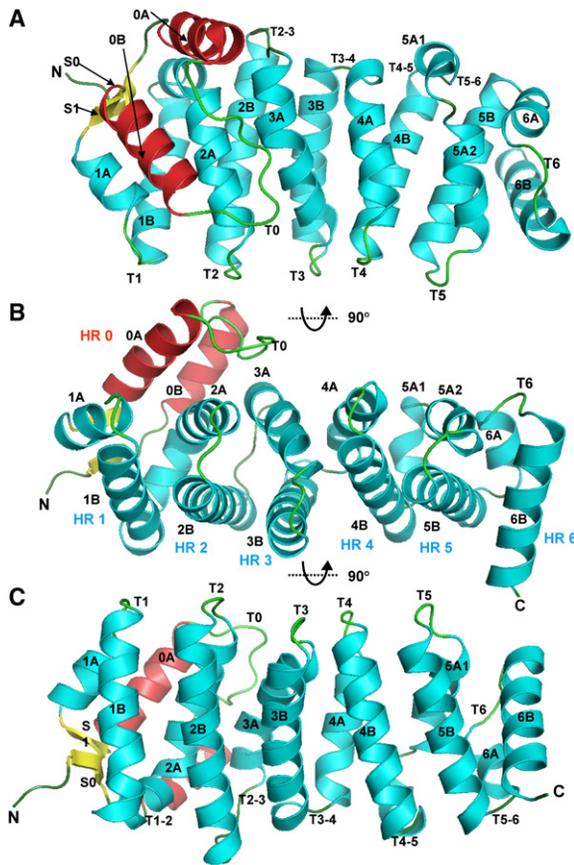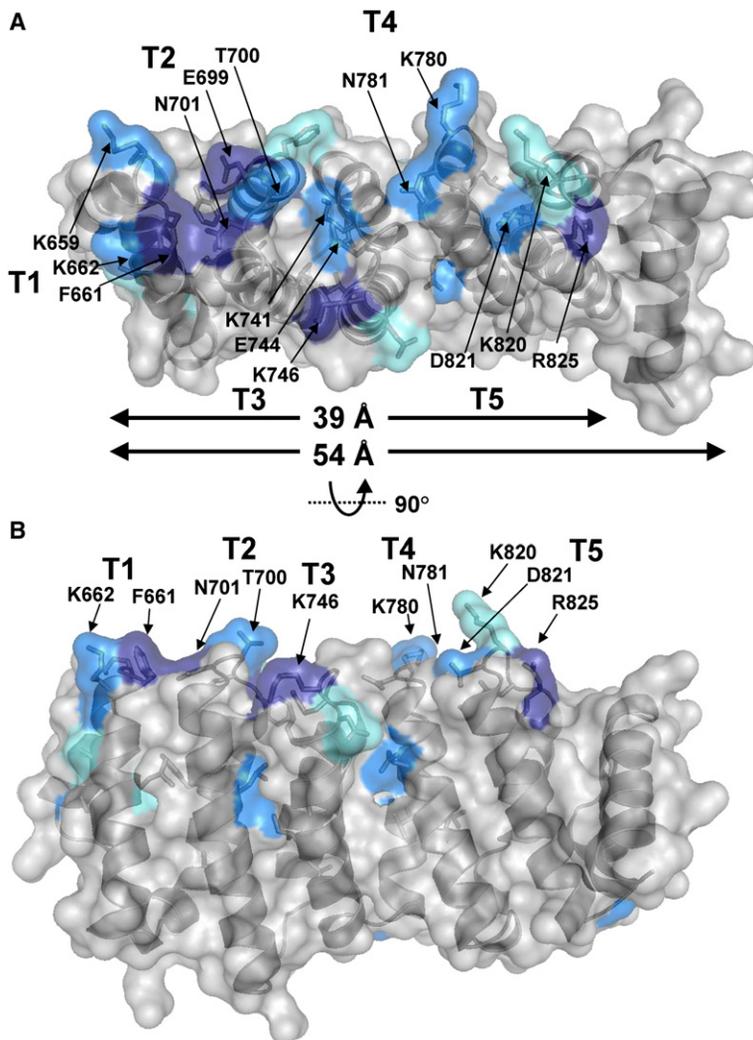
Figure 2. Structure of Zyg9-TOG3

(A) Zyg9 TOG3 has seven HEAT repeats. HR0 contains helices 0A and 0B (red) linked by a 14 residue loop (T0). The six HEAT repeats that follow (blue helices, HR1–HR6) form the conserved TOG domain structure. In this view, the A helices (1A–6A) are in the front, the B helices (1B–6B), in the rear; turns between A and B helices of each repeat (T1–T6) are at the bottom, and interrepeat turns (T2-3 and T3-4) are at the top. The HR5 A helix is broken by a nonhelical linker into helices 5A1 and 5A2. HR6 packs onto HR5 with a right-handed 45° twist. There is a short β-ribbon (yellow strands, S0 and S1) at the N terminus.

(B) As in (A), but viewed from the bottom (structure rotated by 90°).

(C) As in (A), but structure rotated by 180°.

in HR1 through HR6 (Figure 3). Thus, the paddle-like structure we see in Zyg9-TOG3 (blue helices in Figures 2 and 3) appears to represent a true TOG-domain core. Sequence conservation suggests that all TOG domains have six HEAT repeats (Andrade et al. 2001), although a smaller number has been "predicted" for some of them (reviewed by Ohkura et al., 2001). The conservation appears in two groups of residues. First, as in most HEAT-repeat structures, hydrophobic residues within the A and B helices of each repeat are conserved. These residues form the hydrophobic core of the paddle. Second, solvent-exposed residues within or adjacent to the intra-HEAT repeat turns, connecting helix A to helix B in HR1 through HR5, are also conserved (Figure 3, T1–T5). The intra-HEAT repeat turns in other proteins, such as importin-β (Cingolani et al., 1999), are usually shorter than the inter-HEAT repeat
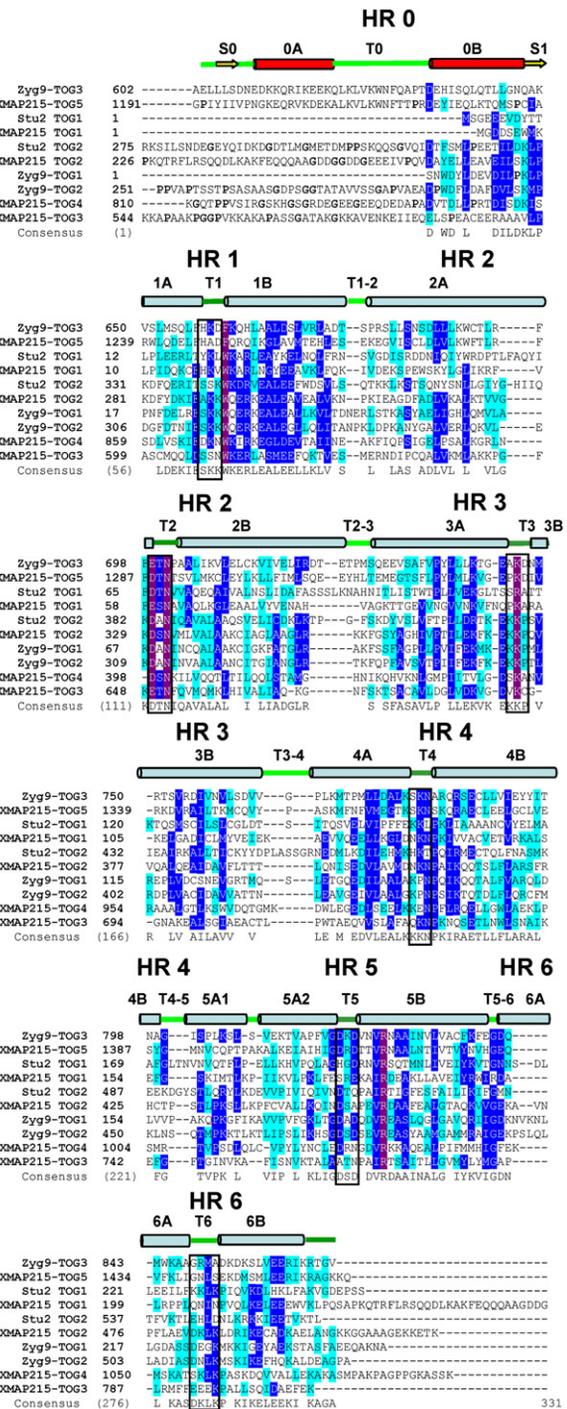
Figure 3. Structure-Sequence Alignment of TOG Domains

Sequences of TOG domains from Stu2p, XMAP215 and Zyg9 (proteins shown in Figure 1), aligned with Clustal W and corrected with pairwise alignments from Psi-Blast (Altschul et al. 1997). Residues invariant within this set are in dark purple; strongly conserved residues, in blue; moderately conserved residues, in light blue. Sequence conservation starts at the end of helix 0B; some TOG sequences (other than Zyg9-TOG3 and XMAP215-TOG5) contain a number of glycines and prolines instead of HR0. The conserved, solvent-exposed residues in the intrahelical turns (T1 through T5) between the A and B helices of the HR1–HR5 are highlighted by boxes.

turns, but they have no particular patterns of conservation. The interrepeat turns in TOG domains (Figure 3, T1-2 through T3-4) are of variable length and sequence (Figure 3), except for the T4-5 and T5-6 turns between HR 4 and 5 and 5 and 6, respectively, which have a single glycine in most cases, and seem to be important for tight packing of those HEAT repeats onto each other (Figure 3).

We mapped the conserved residues in the intrarepeat turns onto the structure, as shown in Figure 4. They lie on a single, narrow face of the TOG domain, forming a patch about 39 Å long. The T1 turn contains the conserved Lys 659, and adjacent conserved residues include Phe 661 and Lys 662 in the 1B helix. These residues are part of a KXWKER motif characteristic of the entire set of TOG sequences, where X represents any type of residue. T2 contains the sequence ETN (residues 699–701), in which Glu699 is highly conserved, Thr 700 is moderately conserved, and Asn 701 is invariant among the domains we analyzed. Conserved residues around T3 include Lys 741 in helix 3A, which projects into the conserved stretch of charge, Glu744, and Lys746. Additional conserved residues in the intrarepeat turns include Lys780, Asn 781

in T4, and Lys820 and Asp821 in T5. Helix 5B contains invariant Arg 825, which projects its guanidinium group toward T5 (Figure 4).

Conserved Residues in the Narrow Face of the TOG Domain Are Required for Tubulin Binding

We have shown, in previous work, that the first TOG domain (TOG1) of budding yeast Stu2 forms a stable molecular complex with tubulin—indeed, sufficiently stable that both components coelute on size-exclusion chromatography (Al-Bassam et al. 2006 and Figure 5A). We mutated conserved residues in the intrarepeat turns of Stu2p-TOG1 to alanine and tested the effects of the mutations on the association of Stu2p-TOG1 and tubulin dimer, by the coelution assay. In T1, we mutated the relatively variable Lys 21 (K659 in Zyg9; Figure 4) and the highly conserved Trp 23 (F661 in Zyg9; Figure 4) in H1B. The elution pattern of the TOG1 K21A mutant in the presence of tubulin resembled that of WT TOG1, whereas the W23A and K21A-W23A double mutant failed to coelute with tubulin dimer (Figure 5A). In T3, mutation of Arg116 (Lys746 in Zyg9; Figure 4) to alanine measurably weakened tubulin
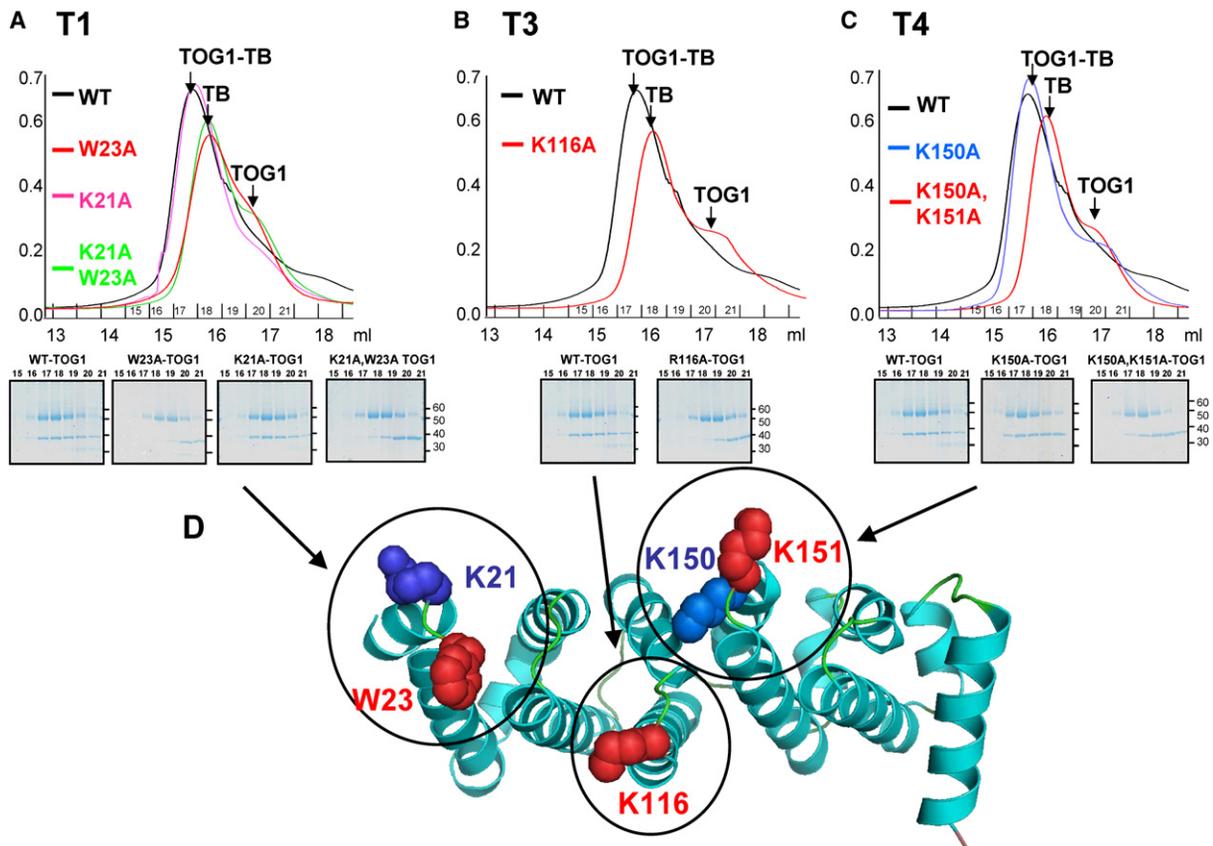
Figure 5. Conserved Residues in the Narrow Face of the TOG Domain Are Required for Binding αβ-Tubulin Heterodimer

(A–C) Effects of mutations in specified residues on the association of Stu2p-TOG1 with tubulin. The upper panels show traces from size-exclusion chromatography on Superose-6; the lower panels, SDS-PAGE analysis of the indicated fractions. Labeled arrows in the upper panels point to peaks corresponding to TOG1-tubulin complex (TOG1-TB), free tubulin heterodimer (TB), and free TOG1 (TOG1), respectively. The data in (A) show the effects of mutations near turn T1. The K21A substitution does not measurably influence coelution of tubulin and TOG1, while the W23A and K21A-W23A TOG1 mutations eliminate coelution almost completely. The data in (B) and (C) show similar analyses of mutations in T3 and T4, respectively.
(D) Positions of the mutated residues with respect to the narrow face of the TOG-domain structure. The structure of Zyg9 TOG3 has been used as a scaffold to display locations of residues in Stu2p-TOG1. Note that W23, K116, and K151—residues shown here to be critical for detectable tubulin binding—project directly toward the viewer, while the less critical residues K21 and K150 project laterally.

binding (Figure 5B). In T4, mutation of Lys 150 (not conserved) to alanine had no detectable effect, while a similar mutation at conserved Lys 151 (residue K780 in Zyg9), which projects from the narrow face of Stu2p, disrupted tubulin binding (Figures 5B and 5C). Thus, a number of residues across the narrow face of TOG domains appear to participate in tubulin binding in solution (Figure 5D). Conservation, as described in the previous section, suggests that there are interactions between tubulin and each of the first five intra-HEAT repeat turns.

Target-protein binding by the narrow face of a HEAT-repeat array may be a common mode of interaction for proteins containing these modules. For example, recently determined structures of protein phosphatase 2A show that conserved residues in the intra-HEAT repeat turns, along one edge of its horseshoe-shaped scaffolding subunit, are critical contacts for capturing its regulatory and catalytic subunits (Cho and Xu, 2007; Xu et al., 2006).

Properties of Different TOG Domains in Dis1/XMAP215 Proteins

Although all TOG domains have the conserved structural features just described, detailed comparisons suggest that they have diverged into types based on their position in the protein (Gard et al., 2004; Al-Bassam et al. 2006). Zyg9-TOG3 represents the C-terminal TOG domain in higher eukaryote family members, which, in addition, have either two or four N-terminal TOG domains (e.g., Zyg9, XMAP215, and MOR1). Experiments with fragments of XMAP215 suggest that those fragments that contain the C-terminal TOG domain (TOG5) may bind the microtubule surface, while the N-terminal TOG domains (TOG1 and TOG2) regulate microtubule dynamics (Popov et al. 2001). Moreover, among the N-terminal domains, the even-numbered ones (i.e., TOG2 and TOG4 in five-domain members, such as XMAP215; TOG2 in two-domain members, such as Stu2p) are more similar to each other than they are to the odd-numbered domains (TOG1 and

Table 1. Crystallographic Statistics for Zyg9 TOG3 Structure

	λ		
	Peak	Inflection	Remote
Wavelength (Å)	0.9795	0.9796	0.9200
Resolution[a] (Å)	30–1.9 (1.95–1.90)	30–1.9 (1.95–1.90)	30–1.9 (1.95–1.90)
Space group	$P4_1$	$P4_1$	$P4_1$
Unique observations	52,652	52,637	52,732
% Completeness[a]	99.8 (99.0)	99.7 (97.9)	99.6 (97.9)
Redundancy	7.4 (5.8)	7.4 (5.9)	7.4 (6.4)
R_{sym}[a,b]	6.1 (41.3)	6.3 (41.9)	6.2 (48.2)
Signal/Noise (I/σ)[a]	41.6 (3.55)	42.2 (3.49)	37.8 (3.29)
Refinement Statistics			
Refined Zyg9-TOG3 atoms (residues)	2,113 (266)		
Refined water molecules	206		
R_{cryst}[c] (%)	17.8 (23.1)		
R_{free}[d] (%)	22.4 (27.2)		
Average B factor (Å^2) Zyg9-TOG3/water	30.5/40.4		
Rmsd bond lengths (Å)	0.021		
Rmsd bond angles (Å)	1.873		
Ramachandran analysis of protein residues[e]	251/15/0/0		

[a] Numbers in parenthesis refer to the highest resolution shell.
[b] $R_{sym} = [\Sigma_h \Sigma_i |I_i(h) - <I(h)>| / \Sigma_h \Sigma_i I_i(h)] \times 100$, where $I(h)$ is the average intensity of i symmetry-related observations of reflections with Bragg index h.
[c] $R_{cryst} = [\Sigma_{hkl} |F_o - F_c| / \Sigma_{hkl} |F_o|] \times 100$, where F_o and F_c are the observed and calculated structure factors.
[d] R_{free} was calculated as for R_{cryst}, but on 5% of data excluded before refinement.
[e] Favored/allowed/generously allowed/disallowed.

TOG3 in XMAP215; TOG1 in Stu2p) (Gard et al., 2004). Indeed, the two different types of TOG domains in Stu2p have different behaviors in vitro. TOG1 binds tubulin with high affinity in solution, whereas TOG2 alone binds very weakly. Nonetheless, both TOG domains are required within the context of a dimeric Stu2p to maintain a stable complex in vitro, and for proper function in vivo (Al-Bassam et al., 2006).

The *stu2* gene was first found as a suppressor of cold-sensitive mutations in β-tubulin (Wang and Huffaker, 1997). Both stu2 alleles originally characterized, designated *stu2-1* and *stu2-2*, are point mutations in TOG2: T514A (*stu2-1*) and D513Y (*stu2-2*). These residues are equivalent to K821 and D820 in T5 of HR5 at one end of the conserved narrow face in Zyg9 TOG3 structure (Figure 4A). The cold-sensitive mutations in β-tubulin that are suppressed by *stu2-1* and *stu2-2* map to solvent-exposed residues I152 and R156, both in helix H4 (see Figure S2 in the Supplemental Data available with this article online; Reijo et al., 1994; Nogales et al., 1998). Stu2p residues 513 and 514, the positions of the suppressor mutations, may therefore contact β-tubulin H4 directly. We suggest that the even-numbered TOG domains (TOG2 and TOG4) bind β-tubulin preferentially, and the odd-numbered domains (TOG1 and TOG3), α-tubulin (see diagram

in Figure S3). These binding preferences can account for the presence in XMAP215/Dis1 family members of alternating domains of each type. Dimeric Stu2p binds a single tubulin heterodimer, and both Stu2p subunits appear to contact tubulin (Al-Bassam et al., 2006). The two TOG2 domains in the dimer must therefore have different interactions, as must the two TOG1 domains. It is possible that, in XMAP215 and other five-domain homologs, the presence of two TOG1-like and two TOG2-like domains within a single polypeptide chain allows them to mimic dimeric Stu2p, but with the two TOG1-like and two TOG2-like elements now somewhat diverged. In the three-domain *C. elegans* Zyg9, TOG1 and TOG2 are both similar to the even-numbered TOG domains of the five-domain proteins (Gard et al. 2004); the nematode family members might dispense with the TOG1-like contacts altogether.

EXPERIMENTAL PROCEDURES

Purification and Crystallization of Zyg9 TOG3
The coding sequence for Zyg9 TOG3 was amplified from a *C. elegans* cDNA library by polymerase chain reaction (PCR) and cloned into a pET21a vector in frame with a C-terminal histidine tag. Selenomethionine (SeMet)-substituted Zyg9 TOG3 was expressed by metabolic labeling in *Escherichia coli* BL21(DE3 plysS) grown in minimal M9

medium supplemented with essential vitamins, nucleotide bases, and amino acids, with Met replaced by SeMet (procedure modified from that of Van Duyne et al., 1993). Expression was induced by IPTG at 27° for 3 hr. SeMet-labeled protein was purified from the bacterial extract with Ni-NTA agarose, followed by size-exclusion chromatography on Superdex-200 (GE Life Sciences), equilibrated in 50 mM Tris, 250 mM NaCl (pH 7.0) (Figure S1). The mass of the purified SeMet-labeled Zyg9 TOG3, determined by liquid-chromatography mass spectrometry, showed 90% replacement of Met by SeMet.

The protein was crystallized in sitting drops mixed with an equal volume of 2.0 M ammonium sulfate, 0.4 M NaCl, 100 mM HEPES (pH 7.5). Crystals grew overnight to 50 μm in all dimensions. Large crystals were transferred to 100 mM HEPES, 1.8 M ammonium sulfate, 8% 2S, 3S-butandiol as cryoprotectant, and flash frozen in liquid nitrogen.

Data Collection and Structure Determination

Multiwavelength anomalous diffraction (MAD) data at three wavelengths were collected at the Advanced Light Source beamline 8.2.2. Reflections with spacings between 30 and 1.9 Å were recorded with a 3Kx3K CCD (Table 1). The three data sets were processed with HKL2000 (Otwinowski and Minor, 1997) in space group P4 (a = b = 54.13 Å, c = 116.63 Å); systematic absences showed the actual space group to be P4$_1$ or P4$_3$. The program SOLVE (Terwilliger, 2003) was used to locate anomalous sites in the P4$_1$ unit cell. Seven high-occupancy sites were found; the initial figure of merit was 0.69. Solvent flattening (applied with the program RESOLVE [Terwilliger, 2003]) yielded a figure of merit of 0.89 at 1.9 Å resolution. The structure was traced with multiple cycles of ARP/wARP (Morris et al., 2003). The initial coordinates were rebuilt with the programs O (Jones et al., 1991) and COOT (Emsley and Cowtan, 2004), followed by refinement with Refmac5 (Murshudov et al., 1997). The final Zyg9 TOG3 model contains residues 602–867, 206 water molecules; R$_{work}$ = 17.8%; R$_{free}$ = 22.4% (Table 1).

Mutagenesis of Stu2-TOG1 and Analysis of Tubulin Binding

The cDNA for TOG1 of Stu2p (residues 1–280) was cloned into a PET28a vector, in frame with a C-terminal histidine tag. Site-directed mutagenesis was carried out with a Gene-Tailor Kit (Invitrogen) with a PCR extension strategy. All mutant TOG1 constructs were confirmed by DNA sequencing. The Stu2p-TOG1 mutant and wild-type proteins were expressed in *E. coli* and purified as previously described (Al-Bassam et al., 2006). To determine tubulin binding, 10 μM of each TOG1 wild-type or mutant protein was mixed with an equal amount of phosphocellulose-purified bovine tubulin dimer and incubated in 100 μl of binding buffer (50 mM HEPES, 180 mM KCl, 1 Mm EGTA, 1 mM MgCl$_2$), and the mixture was then analyzed by size-exclusion chromatography using a 10/5 Superose-6 gel-filtration column (GE Life Sciences), pre-equilibrated with binding buffer; 0.5 ml fractions were collected and analyzed on SDS-PAGE.

Supplemental Data

Supplemental Data, including additional figures, are available online at http://www.structure.org/cgi/content/full/15/3/355/DC1/.

REFERENCES

Al-Bassam, J., van Breugel, M., Harrison, S.C., and Hyman, A. (2006). Stu2p binds tubulin and undergoes an open-to-closed conformational change. J. Cell Biol. *172*, 1009–1022.

Altschul, S.F., Madden, T.L., Schaffer, A.A., Zhang, J., Zhang, Z., Miller, W., and Lipman, D.J. (1997). Gapped BLAST and PSI-BLAST: a new generation of protein database search programs. Nucleic Acids Res. *25*, 3389–3402.

Andrade, M.A., Petosa, C., O'Donoghue, S.I., Muller, C.W., and Bork, P. (2001). Comparison of ARM and HEAT protein repeats. J. Mol. Biol. *309*, 1–18.

Brittle, A.L., and Ohkura, H. (2005). Mini spindles, the XMAP215 homologue, suppresses pausing of interphase microtubules in *Drosophila*. EMBO J. *24*, 1387–1396. Published online March 17, 2005. 10.1038/sj.emboj.7600629.

Cassimeris, L., and Morabito, J. (2004). TOGp, the human homolog of XMAP215/Dis1, is required for centrosome integrity, spindle pole organization, and bipolar spindle assembly. Mol. Biol. Cell. *15*, 1580–1590. Published online January 12, 2004. 10.1091/mbc.E03-07-0544 on.

Charrasse, S., Schroeder, M., Gauthier-Rouviere, C., Ango, F., Cassimeris, L., Gard, D.L., and Larroque, C. (1998). The TOGp protein is a new human microtubule-associated protein homologous to the *Xenopus* XMAP215. J. Cell Sci. *111*, 1371–1383.

Cho, U.S., and Xu, W. (2007). Crystal structure of a protein phosphatase 2A heterotrimeric holoenzyme. Nature *445*, 53–57. Published online November 1, 2006. 10.1038/nature05351.

Cingolani, G., Petosa, C., Weis, K., and Muller, C.W. (1999). Structure of importin-beta bound to the IBB domain of importin-alpha. Nature *399*, 221–229.

Desai, A., and Mitchison, T.J. (1997). Microtubule polymerization dynamics. Annu. Rev. Cell Dev. Biol. *13*, 83–117.

Emsley, P., and Cowtan, K. (2004). Coot: model-building tools for molecular graphics. Acta Crystallogr. D Biol. Crystallogr. *60*, 2126–2132. Published online November 26, 2004. 10.1107/S0907444904019158.

Garcia, M.A., Vardy, L., Koonrugsa, N., and Toda, T. (2001). Fission yeast ch-TOG/XMAP215 homologue Alp14 connects mitotic spindles with the kinetochore and is a component of the Mad2-dependent spindle checkpoint. EMBO J. *20*, 3389–3401.

Gard, D.L., and Kirschner, M.W. (1987). A microtubule-associated protein from Xenopus eggs that specifically promotes assembly at the plus-end. J. Cell Biol. *105*, 2203–2215.

Gard, D.L., Becker, B.E., and Josh Romney, S. (2004). MAPping the eukaryotic tree of life: structure, function, and evolution of the MAP215/Dis1 family of microtubule-associated proteins. Int. Rev. Cytol. *239*, 179–272.

Gergely, F., Draviam, V.M., and Raff, J.W. (2003). The ch-TOG/XMAP215 protein is essential for spindle pole organization in human somatic cells. Genes Dev. *17*, 336–341.

Gräf, R., Euteneuer, U., Ho, T.H., and Rehberg, M. (2003). Regulated expression of the centrosomal protein DdCP224 affects microtubule dynamics and reveals mechanisms for the control of supernumerary centrosome number. Mol. Biol. Cell *14*, 4067–4074. Published online June 13, 2003. 10.1091/mbc.E03-04-0242.

Holmfeldt, P., Stenmark, S., Gullberg, M., Brannstrom, K., and Brattsand, G. (2004). Differential functional interplay of TOGp/XMAP215 and the KinI kinesin MCAK during interphase and mitosis. EMBO J. *23*, 627–637. Published online January 29, 2004. 10.1038/sj.emboj.7600076.

Jones, T.A., Zou, J.Y., Cowan, S.W., and Kjeldgaard, M. (1991). Improved methods for building protein models in electron density maps and the location of errors in these models. Acta Crystallogr. A *47*, 110–119.

Kerssemakers, J.W., Munteanu, E.L., Laan, L., Noetzel, T.L., Janson, M.E., and Dogterom, M. (2006). Assembly dynamics of microtubules at molecular resolution. Nature *442*, 709–712. Published online June 25, 2006. 10.1038/nature04928.

Kinoshita, K., Habermann, B., and Hyman, A.A. (2002). XMAP215: a key component of the dynamic microtubule cytoskeleton. Trends Cell Biol. *12*, 267–273.

Kosco, K.A., Pearson, C.G., Maddox, P.S., Wang, P.J., Adams, I.R., Salmon, E.D., Bloom, K., and Huffaker, T.C. (2001). Control of microtubule dynamics by Stu2p is essential for spindle orientation and metaphase chromosome alignment in yeast. Mol. Biol. Cell *12*, 2870–2880.

Morris, R.J., Perrakis, A., and Lamzin, V.S. (2003). ARP/wARP and automatic interpretation of protein electron density maps. Methods Enzymol. *374*, 229–244.

Murshudov, G.N., Vagin, A.A., and Dodson, E.J. (1997). Refinement of macromolecular structures by the maximum-likelihood method. Acta Crystallographica section D *54*, 1286–1294.

Nakaseko, Y., Goshima, G., Morishita, J., and Yanagida, M. (2001). M phase-specific kinetochore proteins in fission yeast: microtubule-associating Dis1 and Mtc1 display rapid separation and segregation during anaphase. Curr. Biol. *11*, 537–549.

Nogales, E., Wolf, S.G., and Downing, K.H. (1998). Structure of the alpha beta tubulin dimer by electron crystallography. Nature *391*, 199–203.

Ohkura, H., Garcia, M.A., and Toda, T. (2001). Dis1/TOG universal microtubule adaptors—one MAP for all? J. Cell Sci. *114*, 3805–3812.

Otwinowski, Z., and Minor, W. (1997). Processing of X-ray Diffraction Data Collected in Oscillation Mode. Methods Enzymol. *276*, 307–326.

Popov, A.V., Pozniakovsky, A., Arnal, I., Antony, C., Ashford, A.J., Kinoshita, K., Tournebize, R., Hyman, A.A., and Karsenti, E. (2001). XMAP215 regulates microtubule dynamics through two distinct domains. EMBO J. *20*, 397–410.

Reijo, R.A., Cooper, E.M., Beagle, G.J., and Huffacker, T.C. (1994). Systematic mutational analysis of the yeast beta-tubulin gene. Mol. Biol. Cell *5*, 29–43.

Severin, F., Habermann, B., Huffaker, T., and Hyman, T. (2001). Stu2 promotes mitotic spindle elongation in anaphase. J. Cell Biol. *153*, 435–442.

Shirasu-Hiza, M., Coughlin, P., and Mitchison, T. (2003). Identification of XMAP215 as a microtubule-destabilizing factor in *Xenopus* egg extract by biochemical purification. J. Cell Biol. *161*, 349–358.

Terwilliger, T.C. (2003). SOLVE and RESOLVE: automated structure solution and density modification. Methods Enzymol. *374*, 22–37.

Tournebize, R., Popov, A., Kinoshita, K., Ashford, A.J., Rybina, S., Pozniakovsky, A., Mayer, T.U., Walczak, C.E., Karsenti, E., and Hyman, A.A. (2000). Control of microtubule dynamics by the antagonistic activities of XMAP215 and XKCM1 in *Xenopus* egg extracts. Nat. Cell Biol. *2*, 13–19.

Usui, T., Maekawa, H., Pereira, G., and Schiebel, E. (2003). The XMAP215 homologue Stu2 at yeast spindle pole bodies regulates microtubule dynamics and anchorage. EMBO J. *22*, 4779–4793.

van Breugel, M., Drechsel, D., and Hyman, A. (2003). Stu2p, the budding yeast member of the conserved Dis1/XMAP215 family of microtubule-associated proteins is a plus end-binding microtubule destabilizer. J. Cell Biol. *161*, 359–369.

Van Duyne, G.D., Standaert, R.F., Karplus, P.A., Schreiber, S.L., and Clardy, J. (1993). Atomic structures of the human immunophilin FKBP-12 complexes with FK506 and rapamycin. J. Mol. Biol. *229*, 105–124.

Vasquez, R.J., Gard, D.L., and Cassimeris, L. (1994). XMAP from *Xenopus* eggs promotes rapid plus end assembly of microtubules and rapid microtubule polymer turnover. J. Cell Biol. *127*, 985–993.

Wang, P.J., and Huffaker, T.C. (1997). Stu2p: A microtubule-binding protein that is an essential component of the yeast spindle pole body. J. Cell Biol. *139*, 1271–1280.

Whittington, A.T., Vugrek, O., Wei, K.J., Hasenbein, N.G., Sugimoto, K., Rashbrooke, M.C., and Wasteneys, G.O. (2001). MOR1 is essential for organizing cortical microtubules in plants. Nature *411*, 610–613.

Xu, Y., Xing, Y., Chen, Y., Chao, Y., Lin, Z., Fan, E., Yu, J.W., Strack, S., Jeffrey, P.D., and Shi, Y. (2006). Structure of the protein phosphatase 2A holoenzyme. Cell *127*, 1239–1251.

Accession Numbers

Coordinates have been deposited in the PDB with accession code 2OF3.